Kinetics of field evaporation (continuous regime)

A. L. Suvorov, T. L. Razinkova, G. M. Kukavadze, A. F. Bobkov, B. Ya. Kuznetsov, and V. A. Kuznetsov

Institute of Theoretical and Experimental Physics
(Submitted October 22, 1974)
Zh. Eksp. Teor. Fiz. **68**, 1460–1470 (April 1975)

A field-ion microscopy study is made of the kinetics of continuous (electric) field evaporation of the (011) plane of a tungsten specimen at 78 K. Some refinements are introduced into a qualitative model of the process and some parameters of the process are obtained. A program for computer simulation of field-ion images of the surfaces studied in the experiments is devised and realized. The results of the computer calculations are used as the basis for analyzing the experimental data.

PACS numbers: 79.70.

1. INTRODUCTION

The process of low-temperature evaporation of metallic crystals in a strong electric field,[1] first observed with the aid of a field-ion microscope, plays a most important role in ion field-emission microscopy and determines to a considerable degree the success of the entire investigation of the sample at the atomic level. A study of the kinetics of this process makes it possible, in addition, to establish in principle certain physico-chemical properties and parameters of the material. However, the experimental investigation of field evaporation is hindered by a number of factors, the most important among which are: a) the high sensitivity of the field-evaporation rate constant k_{ev} to the change of the electric field intensity F (when F changes by 5% in the field region of direct interest from the practical point of view, k_{ev} increases by more than 10 orders of magnitude); b) the appreciable difference, observed for most materials, between the intensity F_{ev} of the evaporation field and the field F_0 corresponding to the condition of best displaying the sample surface in a given display gas (the maximum of the autoionization probability);[1)] c) the presence of the display gas needed to display the sample of the surface; d) the exceedingly low luminosity of the ion field-emission images.

The analysis of the results is made complicated, furthermore, by the impossibility of establishing with sufficient accuracy the values of F at the surface of the sample (the average field intensity determined in experiment, assuming validity of the Fowler-Nordneim equation in electron field emission,[2] is subject to an error not less than $\pm 15\%$), and more over the local distribution of the field; in addition there is no complete theory of the process.

Certain details of the evolution of field evaporation have been investigated by now experimentally,[3,4] using computer simulation,[5,6] and theoretically in parallel with experiment.[7,8] Brandon[4] obtained for tungsten, molybdenum, and tantalum (all have bcc structure) experimental plots of k_{ev} against F and against the temperature T of the sample under the assumption that the process of field evaporation is thermally activated, and calculated some of its parameters; he paid little attention to the details of the kinetics of the process itself. He also investigated alloys in similar manner.[9] Moore and Spink[7] have studied experimentally the kinetics of the process for the (111) face of tungsten evaporated by field pulses; the results were compared by him with computer-analysis data. Finally, the main result of the work of Vinogradov, Borisov, and Potapov[5,6] was (besides the development of a procedure for computer simulation of the process) a theoretical observation of the anisotropy of field evaporation of a bcc sample oriented along the [110] axis.

Summarizing, we note that the kinetics of field evaporation has not yet been sufficiently well studied, and this seems to pertain to a greater degree to the continuous regime (the field intensity F at the sample surface is maintained constant for a long time, and F is close to the evaporating field F_{ev}—see below), rather than the pulsed regime.

We have investigated experimentally the kinetics of continuous field evaporation of tungsten samples; the results are compared with a theoretical computer analysis.

2. EXPERIMENTAL PROCEDURE AND RESULTS

We investigated samples of commercial tungsten of grade VA-3. The experiments were performed in a highly evacuated dismountable glass field ion microscope[10] provided with an image brightness intensifier[11] based on a three-chamber electron-optical converter of type UM-92. The field-emission images were recorded with an RFK-5 motion-picture camera with "Gelios-40" lens (focal length 80 mm, relative aperture 1 : 2). Typical photographic exposure times ranged from 1/22 to 1/2 sec (optical amplification $\sim 10^3 - 10^4$), and the time of film rewinding was 50 msec. The samples were cooled during the investigation with liquid nitrogen. The study was preceded by a short-duration outgassing heating of the needle-like samples in a vacuum on the order of 5×10^{-8} mm Hg. The display gas was spectrally pure gas at a pressure 1×10^{-3} to 5×10^{-4} mm Hg. The photography was carried out whenever a stable image of the smoothed, field-purified, and highly perfected surface, was observed on the field ion microscope after several atomic sample layers contaminated by the adsorbed gases were removed by the electric field. The sample potential U (and consequently F) was then increased slowly until the microscope screen started to display a contrast change taken to mean a gradual "dissolution" (decrease in diameter followed by complete vanishing) of the displayed annular edges of the crystallographic planes. The increase of U was then stopped, the motion-picture camera was started, and a series of field ion pictures was taken at a fixed $U = U_1 = $ const; this series consisted as a rule of several dozen frames. The potential of the sample was then raised to $U_2 = U_1 + \Delta U$, etc., so long as the speed of the cinematography made it possible to record individual stages of the pro-

cess of removal (evaporation) of the atoms[2] from the surface of the sample.

Notice must be taken here of two essential methodological circumstances that greatly impede the described procedure. First, it is necessary to work with sufficiently sharply pointed samples, so that the values of U_0 and U_{ev} corresponding to the optimal display of the sample surface (U_0) and to the start of its field evaporation (U_{ev}) differ insignificantly from each other. Second, it is necessary that the series of ion-emission images obtained at different U correspond to samples having equal radii and, no less important, that they have surfaces of similar geometric configuration. Failure to satisfy the last condition greatly hinders the already quite approximate comparative estimate of the results; this condition can be satisfied in practice (approximately) in two ways, either by fixing in each run the removal (field evaporation) of only one or two surface layers, or else by working with samples having large r_0. The second procedure, however, contradicts the indicated requirement that U_0 and U_{ev} be nearly equal, and corresponds in addition to a deterioration of the resolution of the apparatus (when the samples are cooled with liquid nitrogen). We have investigated here therefore only thin samples.

Two typical series of field-ion images, describing the kinetics of the field-evaporation of tungsten sam-

ples in the region of the central face (011), are shown in Figs. 1 and 2. The 15 frames of the figure illustrate the (incidentally, incomplete) removal by the field of only one upper plane. The important direct information is the observed anisotropy of the field-evaporation (increased rate of evaporation along the crystallographic directions $[\bar{1}00]-[100]$, which is revealed on the frames by the "elongation" of the initially "round" upper plane along the zone line $[100]$). The latter, as is well known, coincides with the decoration line in tungsten. As shown above, a similar anisotropy was estimated theoretically in[5,6]. The series of images shown in Fig. 2 corresponds to a larger rate of evaporation; during the time of exposure of frames 5, 12, and 14 a "collapse" of the central annular edges of the (011) planes took place, i.e., they were evaporated completely. A total of six upper (011) planes were evaporated in the time between the first and the fifteenth frames (~75 sec).

A very remarkable series is shown in Fig. 3. It shows plots of the kinetics of the field-evaporation of a mound resulting from the detachment of the sharp point at an exposure 1/33 sec and with a time interval 0.1 sec between neighboring frames.[12] These pictures demonstrate not only the sequence in which the atoms

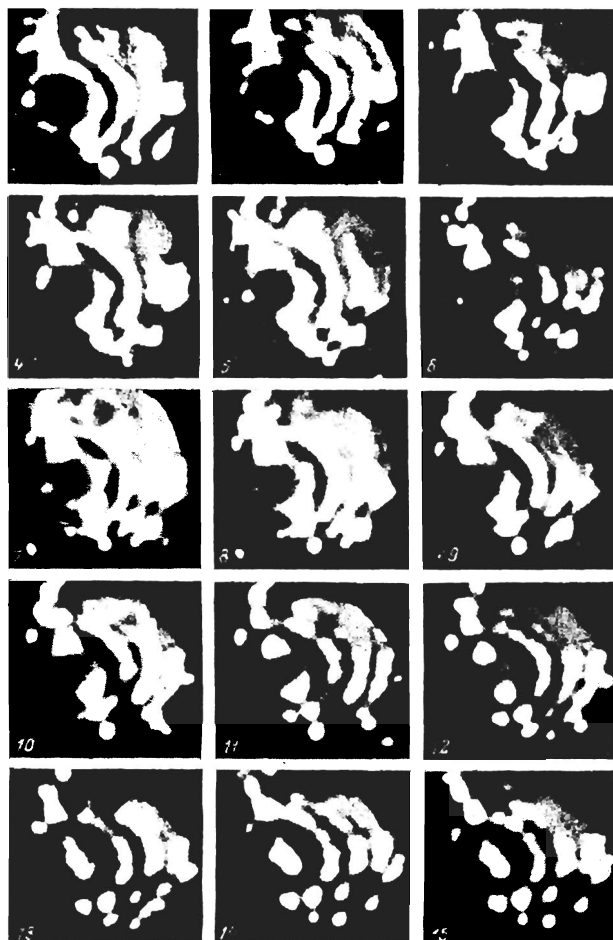

FIG. 1. Kinetics of field evaporation of a tungsten sample in the region of the central face (011); U = 12.6 kV, t_e = 1.5 sec. Anisotropy of field evaporation is observed, viz., "contraction" of the upper plane along $[00\bar{1}]$ and $[001]$ and "dilation" along $[110]$ and $[\bar{1}10]$.
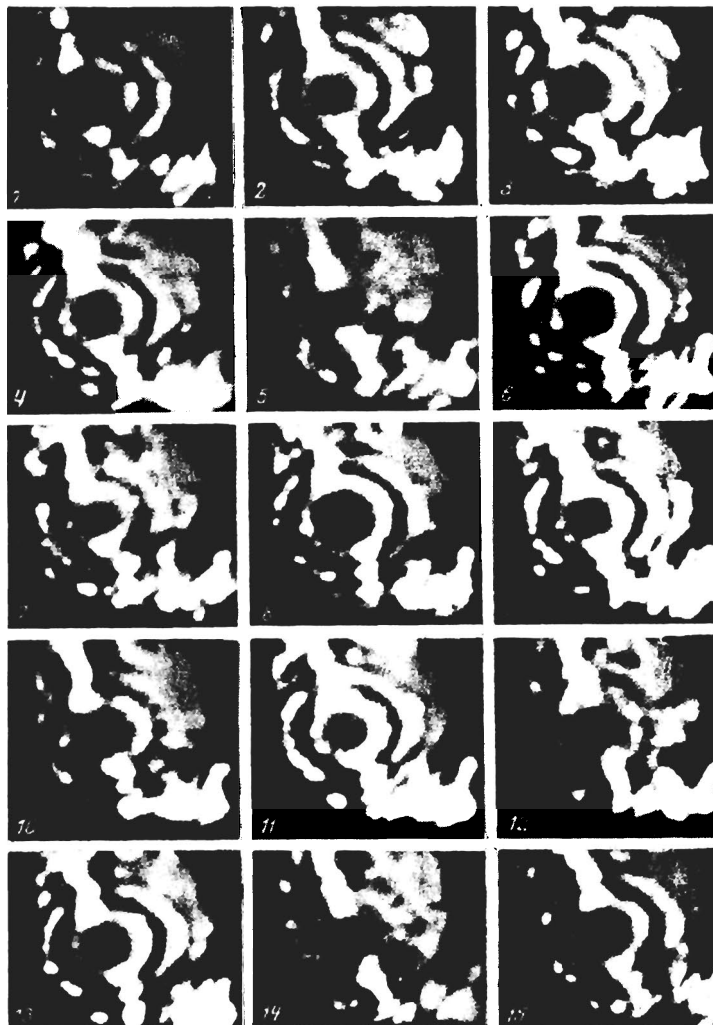

FIG. 2. Kinetics of field evaporation of tungsten sample in the region of the central face (011). U = 11.1 kV, t_e = 5.0 sec. Frames 5, 12, and 14 correspond to "collapse" of the annular edges of the upper plane directly during the time of the exposure.

are removed in the electric field, but also the variations of the local contrast (brightness and dimensions of the spots) in time and as functions of the atomic environment. Indeed, the brightest spot (arrow a on frames 1–4) is produced on the pictures by two surface atoms. Removal of atom b (frame 8) and of atom c (frame 11) also changes the dimensions and the image brightness of the neighboring atoms (c and d). We note that the atom corresponding to spot d (frame 12) seems to be located in the second (011) plane from the top; otherwise it is difficult to explain its relatively high stability compared with the atom that yields spot c. To be sure, one more possible explanation of the observed field-evaporation sequence may be that the appearance of the spot d corresponds to an interstitial or impurity (implanted) atom of a second plane.[13]

The obtained series of the field ion pictures (of the type shown in Figs. 1 and 2) were used to plot the time

dependences of the ring diameter d (of the image of the annular edge) of one and the same plane (Fig. 4). As a rule, the measurements were made in two perpendicular directions. Their analysis shows that there exist several relatively stable configurations (corresponding to horizontal sections of the shown plots), the stable lifetime of which and the evaporation time (the transition to the next relatively stable configuration) of which are connected with their dimensions and geometry, i.e., in final analysis, with the type of bond between their constituent atoms. A major confirmation of this statement is that the distances Δd between any two horizontal sections always turn out to be multiples of the distance between two neighboring spots on the picture of the given plane. Intermediate values of the diameters d (inclined sections of the plots in Fig. 3) correspond to removal of one or several atoms of the analyzed configuration.

3. BRIEF ANALYSIS OF THE PROCESS AND DISCUSSION OF RESULTS

There exist at present several approaches to the analysis of the field-evaporation process. Usually[3] one distinguishes in this process three principal stages making various contributions at different temperatures, viz., thermal excitation, electronic transition, and atomic or electronic tunneling. In [14], furthermore, the indicated process is regarded as a particular case of surface ionization. The limits of applicability of the developed theories were discussed in numerous papers and review articles, but the question has not yet been fully clarified.

It is estimated[14] that for tungsten at $T \geq 70°$ K one can neglect atomic and ionic tunneling and the process itself can be regarded as thermally activated with a rate k_{ev} given by the Arrhenius equation[16]

$$k_{ev} = p\nu \exp \left(-Q_n/kT \right) \quad (\text{sec}^{-1}). \qquad (1)$$

Here p is the probability of electronic transition within a time $1/\nu$, ν is the frequency of the atomic surface oscillations, k is Boltzmann's constant, and Q_n is the activation energy of the process in the field F.

In the case of a metallic bond it is assumed that[17]

$$Q_n = Q_0 - \Delta Q = Q_0 - (n^3 e^3 F)^{1/2} + 1/2 (\alpha_a - \alpha_i) F^2, \qquad (2)$$

where the activation energy Q_0 in the field F = 0 is determined from the thermo-ionic cycle

$$Q_0 = \Lambda + \sum_n (U_{ev})_n - n\varphi, \qquad (3)$$

n is the charge of the evaporated ion (n = 2 for tungsten), $(U_{ev})_n$ is the corresponding ionization potential, φ is the work function, e is the electron charge, α_a and α_i are respectively the polarizations of the atom and the ion, and Λ is the sublimation energy. In connection with the uncertainty in the values of α_a and α_i, for most metals the polarization effects are neglected in the estimates and the lowering ΔQ of the potential barrier in the field F is assumed equal to

$$\Delta Q = (n^3 e^3 F)^{1/2}. \qquad (4)$$

In this paper, certain parameters of the field evaporation of tungsten were estimated under the assumption that the Stranski and Suhrmann ideas[18] concerning the role of the atomic environment, and the possibility of approximating the metallic bond by central forces,
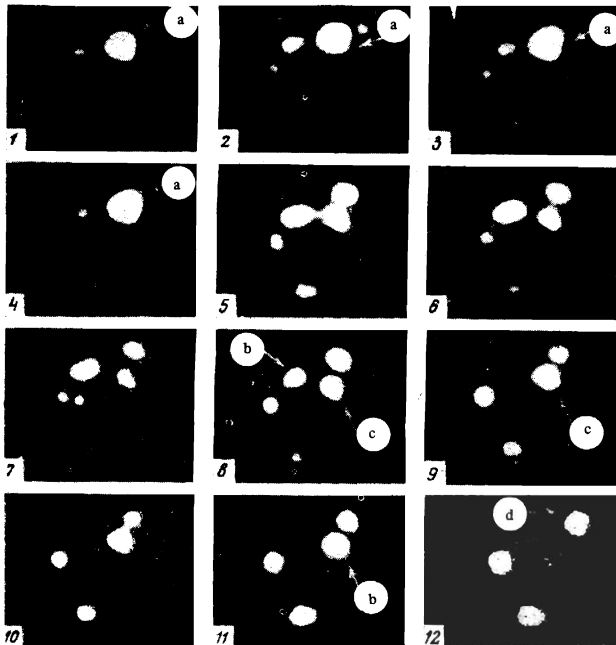

FIG. 3. Sequence of field evaporation of a mound produced on the surface of a tungsten sample when the point of the sample is broken off by the force of the applied electric field.
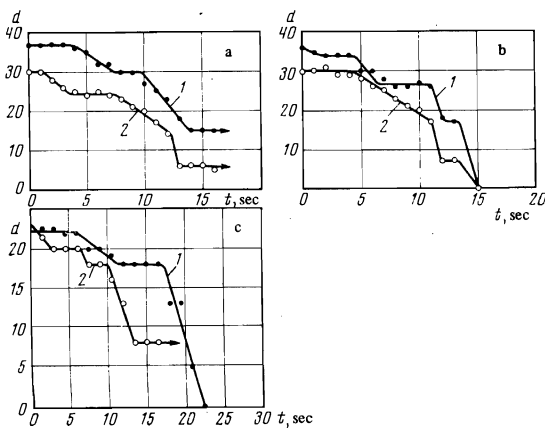

FIG. 4. Typical time dependences of the diameter d (in relative units) of the displayed annular edge of a continuously field-evaporated plane, plotted for two mutually perpendicular directions (curves 1–along [01̄1], curves 2–along [100]). U = 12.6 kV.

are valid. In spite of the obviously limited nature of this concept, its use, as is well known, has already yielded in a number of cases rather satisfactory agreement with experiment, and resulted in certain important theoretical estimates (see, e.g., [19]).

We used the method described in [20-22] to take into account the atomic environment to simulate the ion field-emission images of the defect structures of the crystals. The criterion for the evaporation of an atom in an electric field F was the condition

$$N_{attr} \leqslant N_{attr}{}^k, \tag{5}$$

where the quantity N_{attr} characterizes the binding energy of the atom with a given environment on the sample surface. The choice of N_{attr}^k is discussed in detail in [20], and the atom type itself on the surface of the tungsten sample is discussed in [23,24]. Next, we replaced Q_0 in (2) and (3) by

$$Q_0 = \psi_1 N_{attr}, \tag{6}$$

where ψ_1 is the binding energy of the atom with its nearest neighbor (assumed equal to 4.15 eV).

Figure 5a shows the calculated dependence of the time Δt (in logarithmic scale) of evaporation of an atom with environment[3] $4 \cdot 3 \cdot 6 \cdot 11 \cdot 3$ ($N_{attr} \approx 5.9083$) on F at T = 78° K. Taking into account the exceedingly high sensitivity of Δt to the field F, we calculated also an artificially "roughened" relation, by introducing into the argument of the exponential of (1) a factor η equal to 0.026. The purpose of this "roughening" was mainly to get around a difficulty of technical character in the computer simulation of the process. The quantity Δt, equal to $1/k_{ev}$, can be interpreted as the mean value of the time during which an atom with a given environment stays on the surface in a bound state. The straight line with $\eta = 0.9176$ corresponds to a sample temperature T_{attr} calculated from the experiment and equal to

$$T_{attr} = \frac{[8e^3(F'-F'')]^{1/2}}{k \ln(k_{ev}'/k_{ev}'')}, \tag{7}$$

where k'_{ev} and k''_{ev} are the experimentally determined field-evaporation rate constants at F = F' and F = F'', respectively (the fields were determined from the empirical relation F = U/5r₀, where r₀ is the radius of curvature of the needle point, determined by counting the number of annular edges of the pictures of the crystal planes between two poles.[25] The value of T_{attr} was 85° K.

For absolute estimates we can use the same plots of Fig. 5 by changing from the straight lines correspond-

ing to $\eta = 0.026$ to the lines reflecting the real sample temperature in the ion field-emission microscope. The dependence of Δt on N_{attr} for F = 5.2 V/Å is shown (also in logarithmic scale) in Fig. 5b.[4]

The presented calculations can be used also to explain satisfactorily the experimental results. The observed existence of relatively stable configurations (cf. supra) is due to the strong difference between the times Δt for surface atoms with different environments. The time Δt of the stable existence of a given configuration (the horizontal sections on the plots of Fig. 4) are given, as seen from the estimates, by the time $\Delta t = (\Delta t)_{min}$ corresponding to the surface atom (or atoms) with the weakest binding. The indicated atom (or atoms) can be regarded as a "nucleus" of the evaporation; its (their) evaporation weakens the bonds of the neighboring atoms, the evaporation time Δt of which decreases sharply, etc. Having calculated the relative evaporation times Δt of the surface atoms with typical environment (it is obvious that this relation is qualitatively independent of the field intensity F), and having determined from the real field ion pictures the crystal configuration corresponding to the considered picture of the annular edge of the given plane, we can establish the rate k_{ev} of evaporation of an atom with known surrounding in a field F. This can also be used to solve the inverse problem: on the one hand, we can calculate (estimate) the binding energy of the atom or, on the other hand, knowing (or estimating) its binding energy we can establish the local field intensity F. These estimates can be obtained, unfortunately, only for atoms that are relatively strongly bound to the surface (and correspond to relatively large values of N_{attr}).

4. COMPUTER SIMULATION

Computer simulation of field ion pictures of a field-evaporated tungsten surface in the region of the central (011) face was carried out by us using a special program based on the "thin shell" method[26] and on the approximation of k_{ev} by means of Eq. (1) without allowance for polarization effect. The initial sample radius r₀ was 27.4Å and the thickness of the pictured surface layer r₀ was chosen to be 1.0Å. In addition, the program took into account the local brightness of the images of the individual atoms; to this end, the layer was broken up, as suggested in [13], into four sublayers of equal thickness. Atoms in the upper sublayer produced a brighter spot (of larger diameter) on the model, etc. The values of Δt calculated for the evaporation of each atom were determined from the formula

$$\Delta t = c \exp\left[\eta \frac{10^4}{T}(c_2 N_{attr} + c_1 \sqrt{F})\right], \tag{8}$$

where c = 100, $c_1 = -12.48$, and $c_2 = 4.82$. The sample temperature was T = 78° K, the value of η was chosen, in accord with the considerations given above, to be 0.026, and F = 5.6 V/Å.

One of the examples of the sequence of field evaporation of the (011) face is shown schematically in Fig. 6. The lines on this figure join together image points corresponding to atoms in relatively stable configurations (there are two of them in Fig. 6). At the initial instant of time, the points 1−6 correspond to atoms with environment 0_1 (see Tables I and II, which show also the corresponding evaporation times Δt). The atoms corresponding to spots 1 (we shall call them
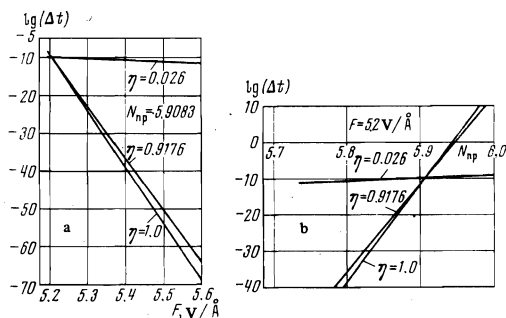

FIG. 5. Theoretical plots of the time Δt of evaporation of the atom with $4 \cdot 3 \cdot 6 \cdot 11 \cdot 3$ bond on the electric field intensity F at the sample surface (a) and on the type of its bond (N_{attr}) in a field F = 5.2 V/Å (b).

A. F. Suvorov et al.

simply atoms 1) are evaporated ~ 1.36 sec[5] after the formation of the initial configuration. At the same time, a change takes place also in the bond between the remaining atoms; the new environment and values of Δt are listed in column 0_2 of the table. After 0.174×10^{-6} sec, atoms 2 are evaporated, and 0.126×10^{-2} sec later, atoms 3. Thus, the average time $(\overline{\Delta t})_1$ for the indicated (first) configuration is determined by the evaporation time of the first atoms, i.e., in the experiment corresponding to this case all the estimates should have been made for atoms with a bond of the $4 \cdot 3 \cdot 6 \cdot 11 \cdot 3$ type. In the produced second configuration the environment corresponds to column 0_4 of Table I. The atoms 4, which are least bound with the surface, are evaporated within ~ 0.55 sec; the resultant new environment is 0_5. The time of evaporation of atoms 5 is 0.9×10^{-7} sec. Consequently $(\overline{\Delta t})_2 = 0.55$ sec and corresponds to atoms with a bond of the type $4 \cdot 3 \cdot 5 \cdot 12 \cdot 2$. It should be noted here that the field-evaporation process is in fact of random
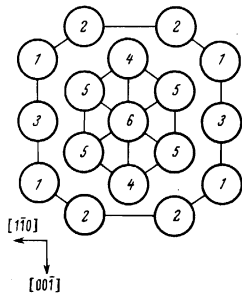

FIG. 6. Sequence of field-evaporation of the upper plane (110) of a tungsten sample.

$[\bar{1}\bar{1}0]$

$[00\bar{1}]$

TABLE I. Atomic environment (type of bond) and values of N_{attr} for atoms in the configurations of the central face (011) of tungsten.

Atoms	Environment					
	0_1	0_2	0_3	0_4	0_5	0_6
1	$4 \cdot 3 \cdot 6 \cdot 11 \cdot 3$ 5.8520	—	—	—	—	—
2	$4 \cdot 3 \cdot 6 \cdot 12 \cdot 3$ 5.8723	$3 \cdot 3 \cdot 6 \cdot 12 \cdot 3$ 4.8723	—	—	—	—
3	$4 \cdot 4 \cdot 6 \cdot 12 \cdot 4$ 6.3098	$4 \cdot 2 \cdot 6 \cdot 12 \cdot 4$ 5.4661	$4 \cdot 2 \cdot 6 \cdot 10 \cdot 4$ 5.4255	—	—	—
4	$6 \cdot 3 \cdot 7 \cdot 12 \cdot 4$ 7.9407	$6 \cdot 3 \cdot 5 \cdot 12 \cdot 4$ 7.8352	$4 \cdot 3 \cdot 5 \cdot 12 \cdot 4$ 5.8352	$4 \cdot 3 \cdot 5 \cdot 12 \cdot 2$ 5.8040	—	—
5	$6 \cdot 4 \cdot 6 \cdot 12 \cdot 4$ 8.3098	$5 \cdot 4 \cdot 6 \cdot 11 \cdot 4$ 7.2895	$5 \cdot 3 \cdot 6 \cdot 11 \cdot 3$ 6.8520	$4 \cdot 3 \cdot 6 \cdot 11 \cdot 3$ 5.8520	$3 \cdot 3 \cdot 6 \cdot 10 \cdot 3$ 4.8318	—
6	$6 \cdot 4 \cdot 7 \cdot 14 \cdot 6$ 8.4344	$6 \cdot 4 \cdot 7 \cdot 14 \cdot 2$ 8.3719	$6 \cdot 4 \cdot 7 \cdot 10 \cdot 2$ 8.2907	$6 \cdot 4 \cdot 5 \cdot 10 \cdot 2$ 8.1853	$6 \cdot 2 \cdot 5 \cdot 10 \cdot 2$ 7.3415	$2 \cdot 2 \cdot 5 \cdot 10 \cdot 2$ 3.3415

TABLE II. Evaporation times t (in seconds) of the atoms in the configurations of the central face (011) of tungsten in a field of intensity F = 5.0 V/Å.

Atoms	Environment					
	0_1	0_2	0_3	0_4	0_5	0_6
1	$3.7 \cdot 10^6$ $2.7 \cdot 10^{-10}$	—	—	—	—	—
2	$1.0 \cdot 10^{14}$ $3.7 \cdot 10^{-10}$	0 $3.9 \cdot 10^{-17}$	—	—	—	—
3	∞ $4.2 \cdot 10^{-7}$	0 $5.5 \cdot 10^{-13}$	0 $2.8 \cdot 10^{-13}$	—	—	—
4	∞ $1.0 \cdot 10^5$	∞ $1.8 \cdot 10^4$	$1.1 \cdot 10^2$ $2.1 \cdot 10^{-10}$	$4.7 \cdot 10^{-7}$ $1.2 \cdot 10^{-10}$	—	—
5	∞ $3.8 \cdot 10^7$	∞ 2.9	∞ $2.6 \cdot 10^{-3}$	$3.7 \cdot 10^6$ $2.7 \cdot 10^{-10}$	0 $2.1 \cdot 10^{-17}$	—
6	∞ $2.8 \cdot 10^8$	∞ $1.0 \cdot 10^8$	∞ $2.8 \cdot 10^7$	∞ $5.1 \cdot 10^6$	∞ 6.6	0 $8.2 \cdot 10^{-28}$

Notes: 1) The first value of Δt corresponds to $\eta = 1.0$, and the second to $\eta = 0.026$. 2) ∞ means $\Delta t > 10^{-30}$ sec, 3) 0 means $\Delta t < 10^{-30}$ sec.

character, i.e., the atoms 1, for example, are not evaporated simultaneously. Then evaporation of one of the atoms (the first), which leads to weakening of the bonds of its neighbors, "operates as a triggering mechanism" for the entire configuration etc. Turning to the data of Table II for $\eta = 1$, we note that they agree qualitatively with the conclusions drawn above for the case $\eta = 0.026$ and a higher value of the field F. However, as seen from this table, in the real case of a field ion microscope experiment, to observe the existence of a second relatively stable configuration it is necessary not only to choose judiciously the working value of the electric field intensity F, but also to ensure an appropriate rate of motion-picture photography of the images.

Figure 7 shows fragments of a series of simulated field ion images of a tungsten sample in the region of the (011) face; the initial central configuration corresponds to the scheme of Fig. 6. They reflect not only the sequence of evaporation of the surface atoms by the field, but also the change of the image contrast in the evaporation process. Notice should be taken of the following essential dependence of the obtained picture of the contrast (but not of the evaporation sequence!) on the chosen method of varying the radius of curvature of the sample surface as the sample becomes evaporated by the field. In the employed calculation program, the value of r_0 was determined from the most salient atom of the surface each time after evaporation of one atom. Thus, the model shown in Figs. 7a and 7b (altogether, 17 models fixing the distance from the surface of at least one atom were printed out between them) corresponds to radii $r_0 - 27.3207$Å, whereas the model of Figs. 7c, 7d, 7e, and 7f correspond to radii $r_0 = 27.1833$, 26.9527, 26.5797, and 26.4384Å, respectively.
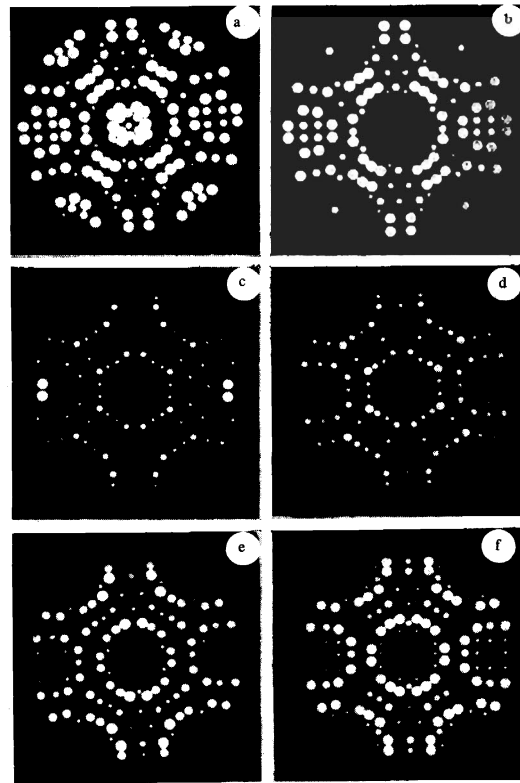

FIG. 7. Fragments from the series of computer-calculated sections of field ion images of a tungsten sample in the region of the central (011) face. The series illustrates the sequence of field evaporation and the corresponding change in the contrast of the field ion images.

On the basis of the foregoing, we can point to three purposes of the assumed computer simulation of the field-evaporation process: a qualitative comparison of the calculated and real field-emission images, reflecting the kinetics of the process; an analysis of the variations of the resultant contrast;, acquisition of quantitative data on the times of stable existence of any particular relatively stable configuration and concerning the type of bond between the atoms that make the decisive contribution to this value. Without disputing the usefulness of the first two, the authors wish to emphasize in conclusion that the most important of the indicated purposes, in their opinion, is the last one. Only in the latter case can the data on the field ion microscopy study of field evaporation in the continuous regime serve as a source of new information (besides the values of $k_{ev}(F)$, $k_{ev}(T)$, etc) on the relative binding energy of atoms having different coordinations on the surface.

---

[1] It should be noted that for the field-ion microscopy procedure itself this difference (at $F_{ev} > F_0$) is, to the contrary, favorable.

[2] It must be borne in mind that in this process the atoms are ionized beforehand, so that strictly speaking it is ions that are removed from the surface.

[3] The first number is that of the nearest atoms ("neighbors" of first order), the second is the number of atoms of second order in distance, etc.

[4] The theoretical value F_{ev} of the evaporating field for tungsten (calculated under the assumption that $Q = (n^3 e^3 F)^{1/2}$, i.e., the evaporation by the field is not in the initial stage, but proceeds already at the high rate $k_{ev} = p\nu$) is 5.5 V/Å; the experimental value if $F_{ev} = 5.7$ V/Å [1].

[5] For clarity and convenience in the qualitative comparison, we present here values corresponding to $\eta = 0.026$ and $F = 5.6$ V/Å.

---

[1] E. Muller and T. Tzong, Field Ion Microscopy, Am. Elsevier, 1969 [Russ. transl., Metallurgiya, 1972].

[2] S. Nakamura, J. Electron Microscopy, 15, 279 (1966).

[3] S. S. Brenner, in High Temperature and Resolution Metallography, Gordon and Breach, N. Y., 1967 p. 1.

[4] D. G. Brandon, Phil. Mag., 14, 803 (1966).

[5] V. V. Vinogradov, V. T. Borisov, and L. P. Potapov, Fiz. Tverd. Tela 15, 649 (1973) [Sov. Phys.-Solid State 15, 460 (1973)].

[6] V. V. Vinogradov, V. T. Borisov, and L. P. Potapov, Fiz. Tverd. Tela 16, 1211 (1974) [Sov. Phys.-Solid State 16, 778 (1974)].

[7] A. J. W. Moore and J. A. Spink, Surface Science, 12, 479 (1968).

[8] A. J. W. Moore and J. A. Spink, Surface Science, 17, 262 (1969).

[9] D. G. Brandon, Surface science, 5, 137 (1966).

[10] V. A. Kuznetsov, G. M. Kukavadze, and A. L. Suvorov, Prib. Tekh, Eksp. No. 2, 152 (1969).

[11] M. M. Butslov, A. F. Bobkov, et al., Prib. Tekh. Eksp. No. 6, 137 (1971).

[12] A. L. Suvorov and G. M. Kukavadze, Fiz. Met. Metalloved. 27, 345 (1969).

[13] L. P. Potapov, T. L. Razinkova, and A. L. Suvorov, Kristallografiya 18, 357 (1973) [Sov. Phys.-Crystallogr. 18, 220 (1973)].

[14] N. I. Ionov, Zh. Tekh. Fiz. 39, 721 (1969) [Sov. Phys.-Tech. Phys. 14, 542 (1969)].

[15] T. T. Tsong, Surface science, 10, 102 (1968).

[16] S. Glasstone et al., Theory of Absolute Reaction Rates (Russ. transl.), IIL (1948).

[17] R. Gomer and L. W. Swanson, J. Chem. Phys., 38, 1613 (1963).

[18] I. Stranski and R. Suhrmann, Ann. der Phys., 1, 169 (1947).

[19] G. N. Shuppe, Élektronnaya émissiya metallicheskikh kristallov (Electron Emission of Metallic Crystals), Izd. SAGU, Tashkent (1956).

[20] A. L. Suvorov, in: Struktura i svoĭstva monokristallov tugoplavkikh metallov (Structure and Properties of Single Crystals of Refractory Metals), Nauka, 1973, p. 52.

[21] A. L. Suvorov and A. G. Sokolov, Kristallografiya 17, 1200 (1972) [Sov. Phys.-Crystallogr. 17, 1052 (1973)].

[22] A. L. Suvorov and A. G. Sokolov, Preprint ITEF-30, 1973.

[23] A. J. W. Moore and D. G. Brandon, Phil. Mag., 18, 679 (1968).

[24] T. L. Razinkova and A. L. Suvorov, Kristallografiya 17, 1217 (1972) [Sov. Phys.-Crystallogr. 17, 1063 (1973)].

[25] E. W. Muller, Adv. in Electronics and Electron Physics 13, 83 (1960)].

[26] A. J. W. Moore, J. Phys. Chem. Solids, 23, 907 (1962).